

350- μ m SHARC-II Imaging of Luminous High- z Radio Galaxies

T.R. GREVE¹, R.J. IVISON^{2,3}, and J.A. STEVENS⁴

¹ California Institute of Technology, Pasadena, CA 91125, USA

² Astronomy Technology Centre, Royal Observatory, Blackford Hill, Edinburgh EH9 3HJ, UK

³ Institute for Astronomy, University of Edinburgh, Blackford Hill, Edinburgh EH9 3HJ, UK

⁴ Centre for Astrophysics Research, Science and Technology Research Centre, University of Hertfordshire, College Lane, Herts AL10 9AB, UK

Received <date>; accepted <date>; published online <date>

Abstract. Using the filled bolometer array SHARC-II on the Caltech Submillimeter Observatory (CSO), we have obtained deep ($\sigma_{rms} \sim 15$ mJy beam $^{-1}$), high-quality 350- μ m maps of five of the most luminous high- z radio galaxies known. In all cases the central radio galaxy is detected at the $\gtrsim 3\sigma$ level, and in some cases the high resolution of SHARC-II (FWHM = 9'') allows us to confirm the spatially extended nature of the dust emission. In PKS 1138–262 ($z = 2.156$), 8C 1909+722 ($z = 3.538$) and 4C 41.17 ($z = 3.792$), additional sources – first discovered by SCUBA at 850- μ m and believed to be dusty, merging systems associated with the central radio galaxy – are detected at 350- μ m. Furthermore, in PKS 1138 and 4C 41.17 additional SHARC-II sources are seen which were not detected at 850- μ m, although the reality of these sources will have to be confirmed by independent submm observations. Thus, our observations seem to support the notion of extended star formation taking place in radio galaxies at high redshifts, and that these systems sit at the centers of overdense regions harbouring a complexity of dusty and vigorously star forming systems. At the redshift of the radio galaxies, the 350- μ m observations sample very close to the rest-frame dust peak (typically at ~ 100 - μ m), and they therefore contribute a particularly important point to the spectral energy distributions of these sources, which we use this in conjunction with existing (sub)millimeter data to derive FIR luminosities, dust temperatures and spectral emissivities of the central radio galaxies.

Key words: cosmology: observations – galaxies: high-redshift – galaxies: formation

©0000 WILEY-VCH Verlag GmbH & Co. KGaA, Weinheim

1. Introduction

High- z Radio Galaxies (HzRGs) are typically identified in low frequency radio surveys as Ultra Steep Spectrum (USS) radio sources (De Breuck et al. 2000), which in conjunction with near-IR colour criteria provide a highly efficient selection scheme. The most powerful ($P_{178MHz} \gtrsim 10^{28} h^{-2} \text{ W Hz}^{-1}$) HzRGs have become an invaluable tool for testing models of galaxy formation, as radio galaxies are amongst the most massive galaxies at all redshifts, and as such they trace out the most biased peak in the primordial density field. Furthermore, owing to their accurate radio positions and morphologies, as well as their extreme properties, such as large (optical) luminosities, extended X-ray and Ly α -halos, HzRGs are relatively easy to study compared to other populations of high- z galaxies.

The first pointed submillimeter (submm) observations of high- z radio galaxies demonstrated that a large fraction of

such systems are extremely FIR luminous ($L_{\text{FIR}} \sim 10^{13} L_{\odot}$) and contain large amounts of dust ($M_d \sim 10^9 M_{\odot}$ – Dunlop et al. 1994; Chini & Krügel 1994; Ivison et al. 1995). Subsequently, systematic 850- μ m surveys with SCUBA of HzRGs by Archibald et al. (2001) and Reuland et al. (2004) confirmed these initial findings, and showed that the dust content of HzRGs increases strongly with redshift. The latter was interpreted as HzRGs being increasingly younger (younger stellar populations) at higher redshifts, since while the FIR luminosities can be powered by either Active Galactic Nuclei (AGN) or starburst activity, the large dust masses requires that vigorous star formation has recently been taking place. Thus, even in HzRGs with their powerful AGNs, starburst activity is likely to contribute substantially to the extreme FIR luminosities, albeit probably less so than in high- z submm-selected galaxies which are predominantly starburst dominated (Alexander et al. 2003). Furthermore, about a handful of HzRGs are known to harbour large reservoirs of molecular gas ($M(\text{H}_2) \sim 10^{11} M_{\odot}$ – e.g. Papadopoulos

et al. 2000; De Breuck et al. 2003; Greve et al. 2004; De Breuck et al. 2005; Klamer et al. 2005) – enough to fuel a $\sim 1000 M_{\odot} \text{ yr}^{-1}$ starburst for $\sim 10^8 \text{ yr}$. Finally, the peak of the dust and CO emission is often not centered on the central radio galaxy, but offset and spatially extended on scale of up to 30-200 kpc. Some of the most striking and visually gratifying examples of this came from submm (850- μm) SCUBA observations of seven high- z radio galaxies, which not only revealed extended ($\sim 30 \text{ kpc}$) dust emission from the central radio galaxy itself, but also showed an overdensity by a factor of two compared to the field of sub-mm sources around the radio galaxies (Stevens et al. 2003), suggestive of extended star formation on hundreds of kilo-parsec scales.

2. Results

Here we present 350- μm lissajou-style scan-maps obtained with SHARC-II (Dowell et al. 2002) on the Caltech Submillimeter Telescope (CSO) on Hawaii of 5 of the 7 HzRGs mapped with SCUBA at 850- μm by Stevens et al. (2003). The motivation for doing this was two-fold: 1) to utilise the superior resolution of SHARC-II (FWHM = 9'') over that of SCUBA (FWHM = 15'') to confirm the spatially extended dust emission from the HzRGs, and the reality of the many companion objects reported by Stevens et al. (2003), and 2) to determine accurate FIR luminosities and dust masses in these objects. SHARC-II observations are particular useful for the latter since at the typical redshift of the HzRGs ($z \sim 3.5$) they probe the $\sim 100 \mu\text{m}$ rest-frame peak of the dust emission. Stevens et al. targeted these 7 sources because they were the brightest sources at 850- μm of the SCUBA observed sample of HzRGs by Archibald et al. (2001). Thus, it is important to keep in mind that our samples represents the most luminous and extreme examples of radio galaxies.

PKS 1138–262 At 350- μm the central radio galaxy (abbreviated RG, and marked by a cross in Figure 1) is seen to be associated with a $\sim 5\sigma$ emission feature consisting of two connected knots roughly aligned with the axis defined by the kiloparsec scale radio jets (marked with tick marks around the central RGs in Figure 1). This double-knotted structure is most likely real since it is also discernable at 850- μm , and in both maps the south-western most source ($S_{350\mu\text{m}} = (92 \pm 18) \text{ mJy}$, $\sim 7''$ south-west from the RG) is the brightest, see Table 1. However, at the position of the RG, which coincided with the weaker knot ($S_{350\mu\text{m}} = (61 \pm 15) \text{ mJy}$), a 1200- μm flux density of $(1.5 \pm 0.5) \text{ mJy}$ was detected using MAMBO on the IRAM 30 m Telescope (Carilli et al. 2001).

The brightest SCUBA source ($S_{850\mu\text{m}} = (7.8 \pm 2.2) \text{ mJy}$) detected by Stevens et al. in this field lies about 70'' east of the RG and coincides with a 1.9σ peak in the 350- μm map. Several explanations may account for the lack of a significant 350- μm detection of this very bright SCUBA source: a) the 850- μm detection could be spurious (it lies at the edge of the SCUBA map), b) the source lies near the edge of the SHARC-II map where the noise is higher which makes it less likely to be detectable, or c) the source is real, but at such a high redshift that the 350- μm band is shifted beyond the dust peak

and samples the SED so far down the Wien tail that it is undetectable given the depth of the maps. We are able to put a 3σ upper limit on its 350- μm flux of $S_{350\mu\text{m}} \lesssim 95 \text{ mJy}$.

Another, much weaker SCUBA source, $\sim 37''$ west of the RG, coincide with $\sim 2\sigma$ peaks in the 350- μm map. We derive an upper limit on its 350- μm flux of $S_{350\mu\text{m}} \lesssim 68 \text{ mJy}$. Finally, a third SCUBA source $\sim 57''$ south of the RG falls outside the 350- μm map. Thus, while we verify the double-knot structure of the central radio galaxy, we do not confirm any of the apparently associated sources seen with SCUBA.

8C 1909+722 The 350- μm SHARC-II map shows a strong ($\gtrsim 5\sigma$) central source ($S_{350\mu\text{m}} = 90 \pm 15 \text{ mJy}$), and a second significant ($\gtrsim 4\sigma$) source about 38'' south-eastwards ($S_{350\mu\text{m}} \sim 148 \pm 32 \text{ mJy}$). The former is offset from the RG-position by $\sim 6''$, while the latter lies within $\sim 8''$ of a strong SCUBA source detected about 46'' south-east of the RG (Stevens et al. 2003). These offsets can easily be accounted for considering that a) we have not corrected for any potential astrometrical offsets between the SHARC-II and SCUBA maps, 2) the beam widths are large (FWHM $\simeq 15''$ in the case of SCUBA), and that c) the two sources are clearly extended at 850- μm .

The RG is marginally resolved at 350- μm , and exhibit the same general shape as seen at 850- μm , thus apparently confirming the claim by Stevens et al. (2003) that the (850- μm) dust emission in this object (and its brightest companion) is extended on tens of kpc scales. This seems to be backed up by the detection of a weak ($\sim 4\sigma$, $S_{350\mu\text{m}} = 70 \pm 17 \text{ mJy}$) source only $\sim 19''$ north-east of the RG, and thus within the north-east extended 850- μm emission from the RG.

A third much fainter SCUBA source, $\sim 35''$ west of the RG and within the SHARC-II map, is not detected at 350- μm , and an upper flux limit of $S_{350\mu\text{m}} \lesssim 28 \text{ mJy}$ is derived.

4C 60.07 This source received by far the least amount of integration time of the 5 HzRGs observed with SHARC-II, and as a result the source is only just detected at the $\sim 3\sigma$ level ($S_{350\mu\text{m}} = 59 \pm 22 \text{ mJy}$). This source was one of the strongest sources detected at 850- μm by Stevens et al. and even showed some, albeit marginal, evidence of being extended. A faint 850- μm source found $\sim 30''$ north of the RG coincides with extended 3σ emission in the SHARC-II map. However, given its small 850- μm flux ($S_{350\mu\text{m}} = 5.9 \pm 1.3 \text{ mJy}$), and the somewhat larger noise level in that part of the SHARC-II map, we do not consider this source robustly detected at 350- μm . We derive a 3σ upper flux limit of $S_{350\mu\text{m}} \lesssim 91 \text{ mJy}$.

4C 41.17 With 5 sources detected at $\gtrsim 5\sigma$ significance, this is by far the richest field observed at 350- μm . All three SCUBA sources detected by Stevens et al., including the RG which even appears to be slightly extended, are detected at 350- μm , and their flux densities are listed in Table 1. Ivison et al. (2000) reported an additional three faint SCUBA sources. However, only one of those sources lies within the SHARC-II map and is not detected to a 3σ limit of $S_{350\mu\text{m}} \lesssim 67 \text{ mJy}$.

The most significant ($\sim 8\sigma$) 350- μm source lies $\sim 53''$

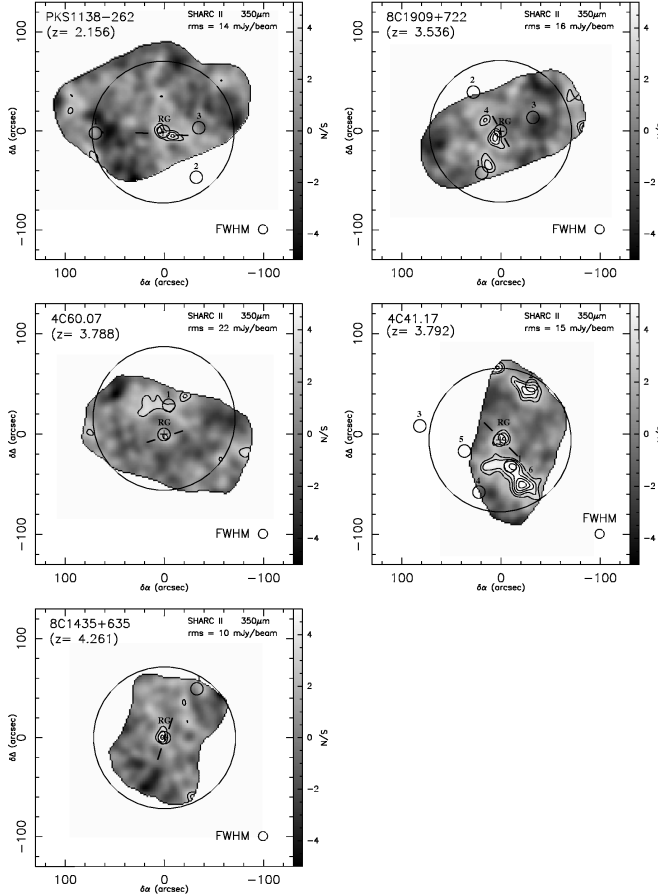


Fig. 1. SHARC-II 350- μ m signal-to-noise maps of the five radio galaxies observed. Contours are at 3, 4, 5, 6 σ , where σ is the rms noise in each map, see the individual panels. The SHARC-II beam at 350- μ m (FWHM = 9'') is shown in the lower right corner of each panel. The crosses mark the position of the radio core. The open circles and the associated labels indicate the 850- μ m sources detected with SCUBA by Stevens et al. (2003) and Ivison et al. (2000). The tick marks around the central radio galaxy indicate the alignment of the large-scale radio jets, and the large circles outline the extend of the SCUBA maps of Stevens et al. (2003).

south-west of the RG, and although it is not detected at 850- μ m it appears to be associated with the very bright SCUBA (and SHARC-II) source $\sim 30''$ north-east of it. The two 350- μ m sources make up a large, extended structure aligned along the jet-direction. The reality of this structure, and of the most south-western source in particular, will have to be confirmed by independent submm observations. Finally, a $\sim 5\sigma$ source is detected at 350- μ m, about 68'' north of the RG. Unfortunately, the source lies outside the SCUBA map and thus cannot be confirmed at 850- μ m. Given that this source lies right at the map edge where the noise is higher, we suspect that it may be spurious.

Although, we cannot exclude that some of the SHARC-II sources (in particular the ones closest to the map edges) are spurious, the confirmation of the three SCUBA sources reported by Stevens et al. (2003), supports their conclusions that the environment of 4C 41.17 has an overdensity of submm sources.

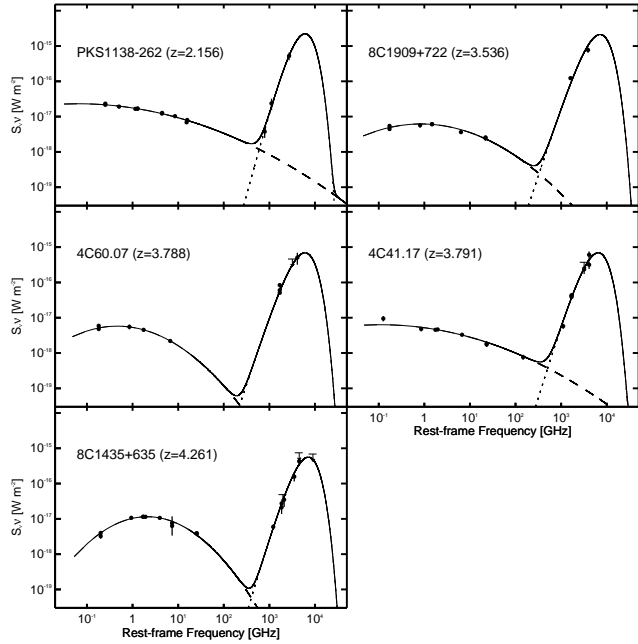


Fig. 2. Radio-FIR/submm spectral energy distributions of the 5 HzRGs observed with SHARC-II. The dust temperature and spectral index were allowed to vary freely in the fitting process, except in the case of 8C 1909+722 where β was fixed at 1.0 due to the small number of data point. The radio part of the spectrum was fitted with a parabola (dashed curves). The combined radio to FIR/submm SEDs are shown as solid curves.

8C 1435+635 Despite being the faintest radio galaxy at 850- μ m, the central radio galaxy is clearly detected ($\gtrsim 5\sigma$) in the SHARC-II maps ($S_{350\mu m} = 51 \pm 9$ mJy). Similar to Stevens et al., who failed to resolve the galaxy at 850- μ m, there is no evidence of extended emission at 350- μ m either, suggesting that this source may be relatively compact. The only other SCUBA source detected in the 8C 1435+635 field lies about 60'' north-west of the RG and coincides with faint 2 σ emission at 350- μ m. We derive an upper flux limit of $S_{350\mu m} \lesssim 68$ mJy.

3. Spectral Energy Distributions, FIR luminosities and Dust Masses

For each of the central radio galaxies, an optically thin grey-body spectrum of the form $S_\nu \propto \nu^{3+\beta} (e^{h\nu/kT_d} - 1)^{-1}$, was fitted using all FIR/submm data points available in the literature. In all cases but 8C 1909+722 more than one independent 850- μ m SCUBA measurement existed (Ivison et al. 1995, 1998; Hughes et al. 1997; Archibald et al. 2001, Reuland et al. 2004), all of which were included in the fitting-process, and in a few cases even 1200-, 450- and/or 350- μ m observations had been made. In the case of 8C 1909+722 where the FIR/submm SED has been sampled at only two separate frequencies we allowed only T_d to vary in the fit for fixed values of $\beta = 1.0, 1.5$ and 2.0 . The best fit was found for $\beta = 1.0$. The resulting dust SEDs are shown as dotted curves in Figure 2, and the fitted T_d and β values are listed in Table 1. The radio part of the spectrum was fitted with a parabolic function

Table 1. Observed 350-, 450-, 850- and 1200- μm fluxes and derived properties of the 5 HzRGs and their associated submm sources (which fall within the SHARC-II maps). The numbering follows that of Stevens et al. (2003) and Ivison et al. (2000).

Source	z	$S_{350\mu\text{m}}^a$ [mJy]	$S_{450\mu\text{m}}^b$ [mJy]	$S_{850\mu\text{m}}^c$ [mJy]	$S_{1200\mu\text{m}}^d$ [mJy]	T_d [K]	β	L_{FIR} [$\times 10^{13} L_{\odot}$]	M_d [$\times 10^8 M_{\odot}$]
PKS 1138–262a	2.156	61 ± 15	...	3.7 ± 2.4	1.5 ± 0.5^e	49 ± 6	1.9 ± 0.2	2.1 ± 0.5	2 ± 1
PKS 1138–262b	2.156	92 ± 18	...	3.8 ± 2.4
1.	...	≤ 95	...	7.8 ± 2.2
3.	...	≤ 68	...	2.2 ± 1.4
8C 1909+722	3.536	90 ± 15	...	34.9 ± 3.0	...	69 ± 3	1.0^e	5.7 ± 0.9	13 ± 2
1.	...	148 ± 32	...	23.0 ± 2.5
3.	...	≤ 28	...	4.3 ± 2.1
4.	...	70 ± 17
4C 60.07	3.788	59 ± 22	69 ± 23	23.8 ± 3.5	...	58 ± 8	1.0 ± 0.2	2.9 ± 1.1	15 ± 6
1.	...	≤ 91	...	6.3 ± 2.1
4C 41.17	3.791	71 ± 17	35.3 ± 9.3	12.0 ± 2.3	2.7 ± 0.3	60 ± 3	1.3 ± 0.1	4.1 ± 0.9	8 ± 2
1.	...	108 ± 17	34.1 ± 9.3	21.2 ± 2.9
2.	...	184 ± 34	...	6.2 ± 1.9
4.	...	≤ 67	≤ 26	2.8 ± 0.8
6.	...	197 ± 24	...	≤ 5
7.	...	181 ± 40
8C 1435+635	4.261	51 ± 9	23.6 ± 6.4	6.0 ± 2.1	...	64 ± 5	1.4 ± 0.1	3.8 ± 0.7	4 ± 1
1.	...	≤ 68	...	3.9 ± 1.8

^a The total flux density within a $r = 15''$ aperture. The flux errors include the ~ 15 per-cent calibration uncertainty; ^b 450- μm flux densities are from Archibald et al. (2002) and Ivison et al. (2000); ^c 850- μm flux densities are from Stevens et al. (2003), except for PKS 1138–262a and b which are our own measurements, and 4C 41.17-4 which is from Ivison et al. (2000); ^d 1200- μm flux densities are from Chini & Krügel (1994) and Carilli et al. (2001); ^e Fixed value.

(dashed curves), and the combined FIR/submm-radio SED is shown as solid curves in Figure 2.

Due to the fact that our 350- μm observations probe the SEDs near their peaks at ~ 100 - μm rest-frame wavelengths, we are able to constrain dust temperatures and FIR luminosities much better than previously. In general, the derived dust temperatures are rather high (lowest value is $T_d = 49$ K), compared to the median dust temperatures of submm-selected galaxies ($T_d \sim 36$ K – Chapman et al. 2004). While HzRGs, in contrast to SMGs where the AGN rarely plays a dominant role (Alexander et al. 2003), harbour powerful AGN, capable of heating the dust in the nuclear regions to high temperatures, it is difficult to envisage them doing so on scales of $\gtrsim 10$ kpc as suggested by the extended 350- μm emission. The spectral emissivity index varies between $\beta \sim 1 - 2$, a similar range to what is observed in SMGs. We note that for objects at $z \sim 3$, β is much better constrained by 850- and/or 1200- μm observations which probe further down the Rayleigh-Jeans tail than 350- μm .

FIR-luminosities obtained by integrating the FIR/submm SED over the wavelengths range 200 – 1000 μm range are listed in Table 1, along with dust masses derived from the observed 350- μm fluxes using a mass absorption coefficient of $\kappa(\nu_r) = 0.11(\nu_r/352\text{GHz})^{\beta}$ in units of $\text{m}^2 \text{kg}^{-1}$. Assuming that only half of the FIR-luminosity in these objects is due to star formation, we find that on average they form stars at a rate of $\sim 1500 M_{\odot} \text{ yr}^{-1}$. The large dust masses suggest that star formation must have been going on for some time in these systems. That such large star formation rates can be sustained for a long enough time to form a giant elliptical (~ 1 Gyr) is shown in the cases of 4C 60.07 and 4C 41.17 where the detection of CO has revealed large amounts of

molecular gas ($\sim 10^{11} M_{\odot}$ – Papadopoulos et al. 2000; Greve et al. 2004; De Breuck et al. 2005).

4. Concluding Remarks

To conclude, our SHARC-II maps confirm the over-densities of dusty galaxies detected in HzRG fields by SCUBA. Furthermore, the superior spatial resolution of these data allow us to confirm that dust emission associated with both the HzRGs and companions is extended on galaxy-wide scales. Our results suggest that mergers play a key role in the formation of these galaxies.

References

- Archibald, E.N.: 2001, MNRAS, 323, 417.
- Alexander, D.M., et al.: 2003, AJ, 125, 383.
- Carilli, C.L., et al.: 2001, ASPC, 240, 101.
- Chini, R. & Krügel, E.: 1994, A&A, 288, L33.
- De Breuck, C., et al.: 2000, A&AS, 143, 303.
- De Breuck, C., et al.: 2003, A&A, 401, 911.
- De Breuck, C., et al.: 2005, A&A, 430, L1.
- Dunlop, J.S., et al.: 1994, Nature, 370, 347.
- Greve, T.R., Ivison, R.J., Papadopoulos, P.P.: 2004, A&A, 419, 99.
- Hughes, D.H., Dunlop, J.S., Rawlings, S.: 1997, MNRAS, 289, 766.
- Ivison, R.J.: 1995, MNRAS, 275, L33.
- Ivison, R.J., et al.: 1998, ApJ, 494, 211.
- Ivison, R.J., et al.: 2000, ApJ, 542, 27.
- Klamer, I.J., et al.: 2005, ApJ, 621, L1.
- Papadopoulos, P.P., et al.: 2000, ApJ, 528, 626.
- Reuland M., et al.: 2004, MNRAS, 353, 377.
- Stevens, J.A., et al.: 2004, Nature, 425, 264.